

Submitted Manuscript: Confidential

template updated: February 2022

Title: Systematic evaluation of neoepitope predictions challenge clinically observed T cell responses and their impact on immune evasion

Authors: Badeel Kh. Q. Zaghla¹, Zuhaf Safyürek¹, Daniela Gröger¹, Shima Mecklenbräuer¹, Nina Lingstädt¹, Johanna Spengler¹, Oliver Popp², Mohamed Haji², Meagan Montesion³, Lee A. Albacker³, Philip Mertins^{2,4}, Martin G. Klatt^{*1,4,5}

Affiliations:

¹Department of Hematology, Oncology and Tumor Immunology, Campus Benjamin Franklin, Charité- University Medicine Berlin; Berlin, Germany.

²Proteomics Platform, Max Delbrück Center for Molecular Medicine; Berlin, Germany.

³Foundation Medicine, Inc.; Boston, Massachusetts.

⁴Berlin Institute of Health (BIH); Berlin, Germany.

⁵German Center for Translational Cancer Research (DKTK), DKFZ; Heidelberg, Germany.

*Corresponding author. Email: martin.klatt@charite.de

One Sentence Summary: Neoepitope predictions only validate for 22% of HLA ligands which often challenges their link to HLA loss and the interpretation of responses to neoantigen vaccines

Abstract: Peptide presentation on human leukocyte antigens (HLAs) is essential for initiating T cell responses and all consequences of this presentation including anti-cancer immunity or immune escape. Many studies have relied on *in silico* prediction tools rather than biological measurement of HLA presentation to study these effects. To better assess the frequency and consequences of neoantigen presentation, we overexpressed 125 combinations of full-length neoantigens and one HLA class I allele to experimentally validate presentation of mutated and non-mutated HLA ligands through HLA ligand isolation followed by tandem mass spectrometry. Successful presentation was observed only in 22% of predicted cases with strong implications on previously described downstream effects. For example, the association of HLA loss of heterozygosity with predicted neoepitopes was challenged for 58% (73/125) of combinations. Furthermore, when testing 51 sequences used for personalized mRNA neoepitope vaccines, we observed that clinical responses were independent of the presentation status of the neoepitopes. Even a presumably neoepitope-specific and strongly expanded TCR clone from a neoantigen vaccination study could not be linked to a successfully presented neoepitope. Overall, these data highlight the importance of validating the presentation of neoepitopes to fully understand our interpretation of clinical mutation-specific responses and their related effects, including immune evasion.

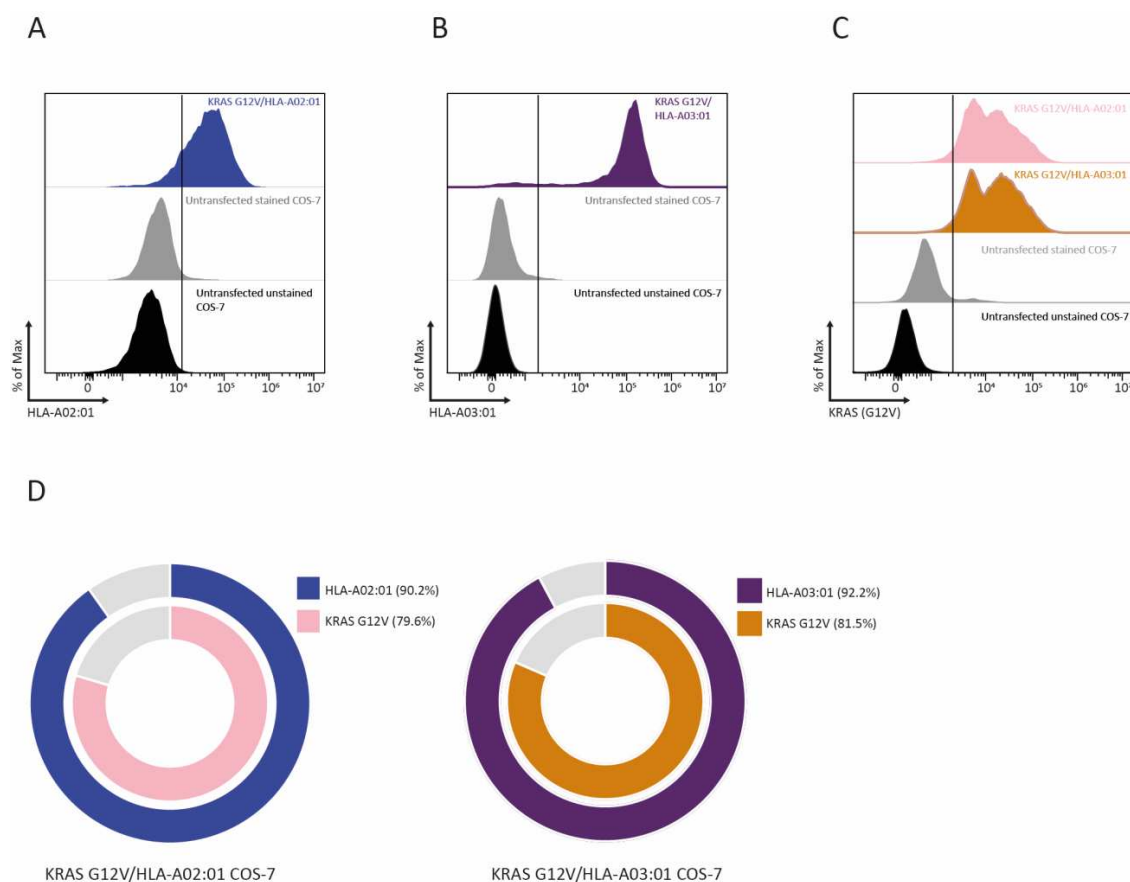


Figure S1: Transfection efficiency of KRAS G12V and representative HLA alleles (HLA-A*02:01 and HLA-A*03:01) in COS-7 cells. (A–C) Representative flow cytometry histograms showing intracellular KRAS (G12V) expression and surface HLA expression in COS-7 cells transfected with KRAS G12V and either HLA-A*02:01 or HLA-A*03:01. Unstained and stained untransfected COS-7 cells were used as negative controls. (A) HLA-A*02:01 expression. (B) HLA-A*03:01 expression. (C) KRAS (G12V) expression. (D) Donut plots showing the percentage of KRAS (G12V) positive cells (inner ring) and HLA-expressing cells (outer ring) for KRAS G12V/HLA-A*02:01 (left) and KRAS G12V/HLA-A*03:01 (right) transfected COS-7 cells.

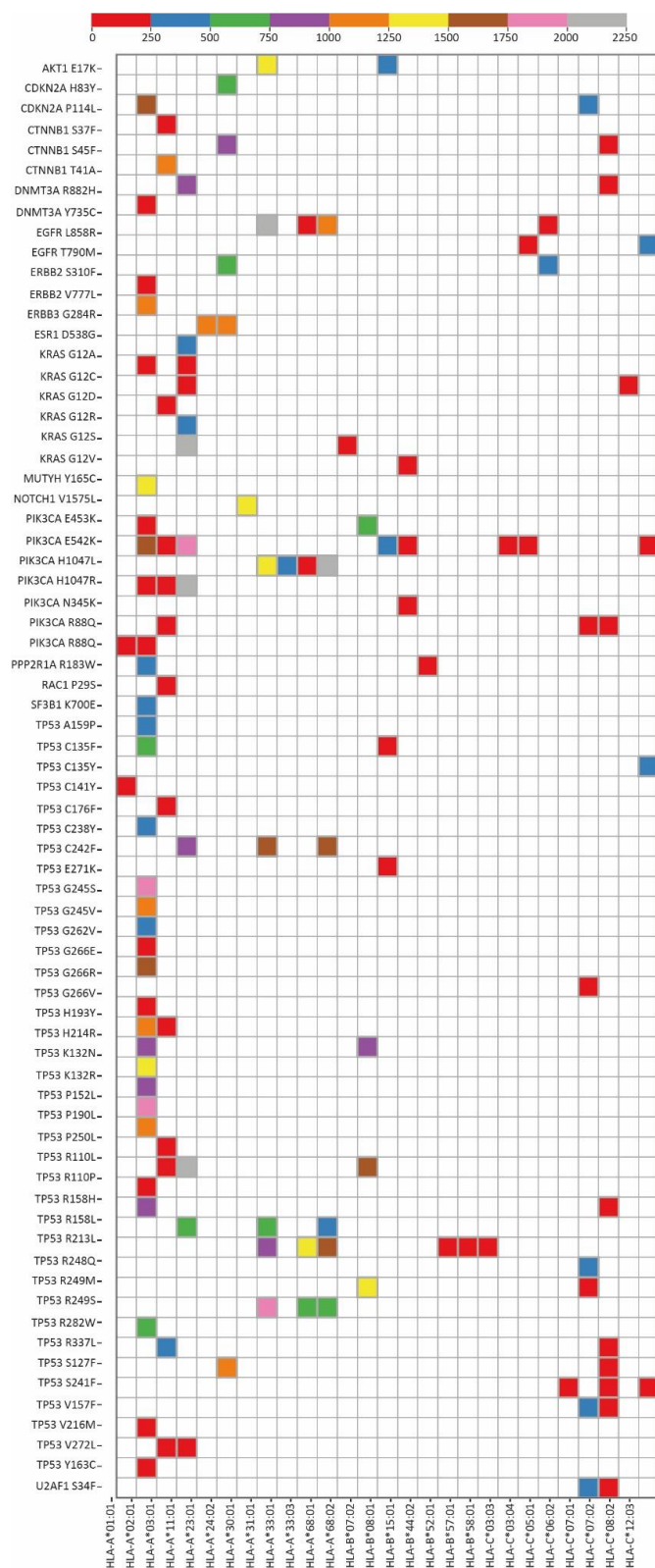


Figure S2: Overview of HLA ligands derived from endogenous and transfected proteins but presented only on the transfected HLA allele. Heatmap showing the number of detected peptides for each combination of HLA allele and neoantigen. The data included peptides derived from both transfected proteins and endogenously expressed COS-7 monkey genes. Only unique peptides meeting the following criteria were considered: a false discovery rate of 5%, a length between 8 and 15 amino acids, and a positive binding prediction by netMHC (EL Rank% ≤ 2). The color bar represents the range of peptide numbers, with varying colors corresponding to different peptide quantities.

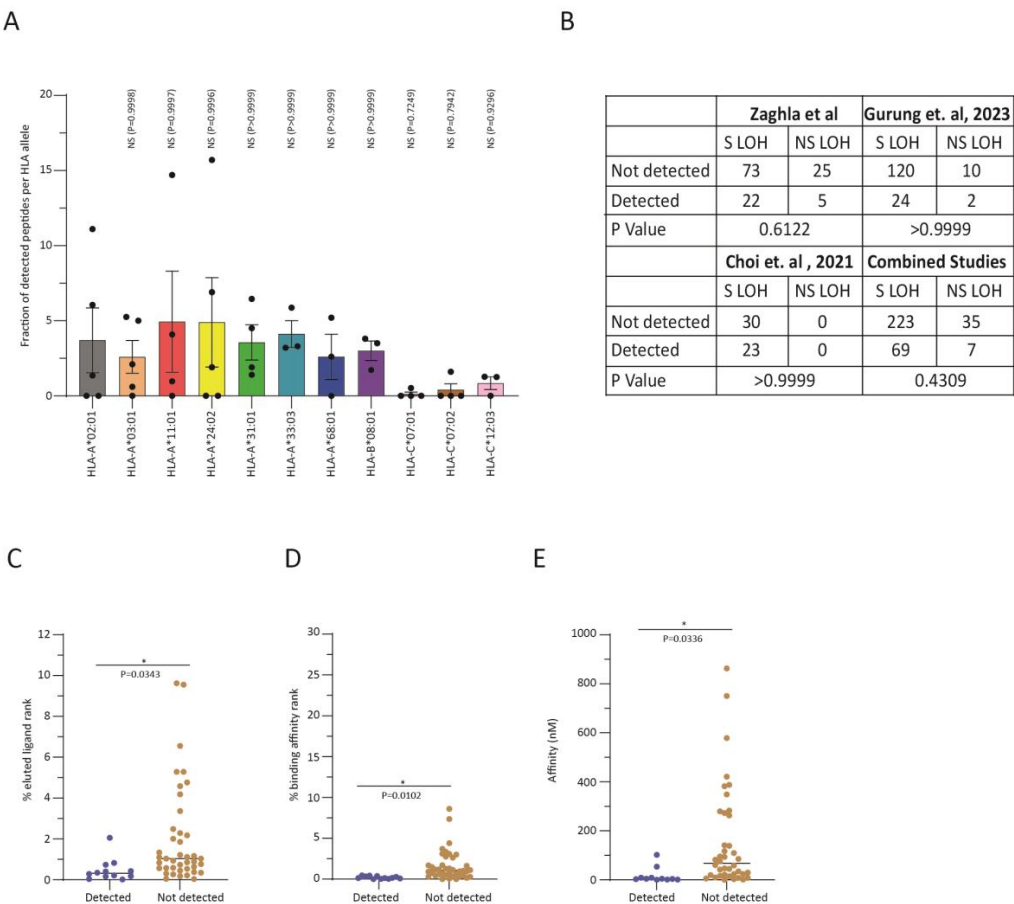
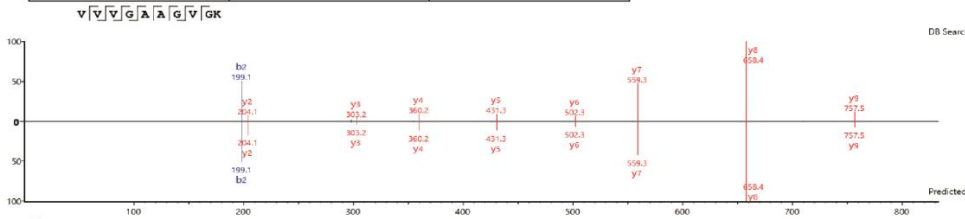
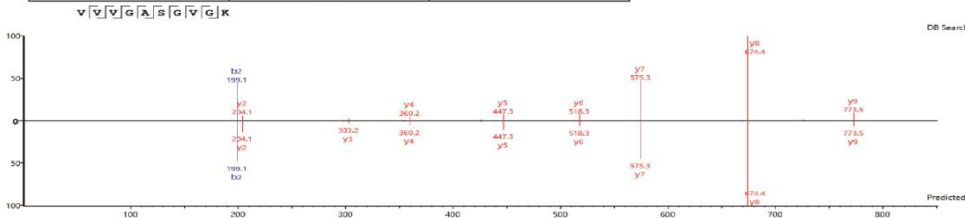


Figure S3: Overview of HLA ligand predictions and neoantigen classification. (A) Bar diagram to compare success rate of peptide detection between HLA alleles. We calculated the number of MS-detected mutated and unmutated peptides compared to predicted HLA ligand for all neoantigen/HLA combinations for which a neoantigen (regardless of its mutation) was at least tested in combination with three different HLA alleles. One-Way ANOVA test was performed for multiple comparisons, using HLA-A*02:01 as the control for the analysis. (B) Correlation of private neoepitope presentation status with reported HLA-LOH across different studies. We identified combinations of HLA alleles and neoantigens that were investigated in the study by Montesion et al. (4) to be associated with significant (S LOH) or non-significant HLA-LOH (NS LOH) and matched these with the presentation status of neoepitopes report in this study (Zaghla et al.), Choi et al. (2021), and Gurung et al. (2023). Fisher's exact test was used to assess the correlation between HLA LOH and neoepitope detection. P-values are provided to indicate statistical significance for each comparison. (C-E) Complimentary analysis to Figure 1D-1I for private neoepitopes. Differences in prediction scores for detected and non-detected (=only predicted) HLA ligands. All scores were obtained by netMHCpan 4.1. (C) eluted ligand (EL) rank refers to a relative scoring trained on immunopeptidome datasets, whereas binding affinity (BA) rank in (D) is a relative scoring matrix based on affinity measurements between peptides and HLA complexes. In (E) we used absolute binding affinity predictions (IC50 in nM) as defined by netMHCpan 4.1. Unpaired Student's t-test was performed for statistical comparison. NS: not significant, *P < 0.05.

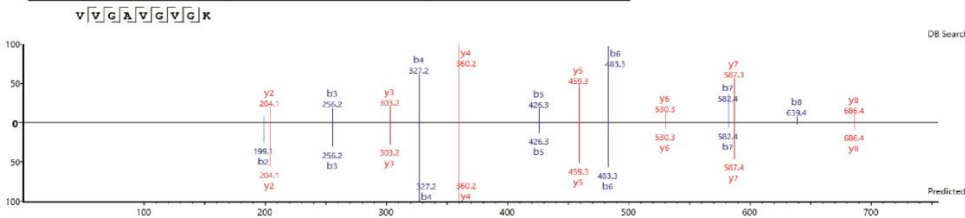
HLA Allele	Mutated Peptide	Mutated Gene
HLA-A*11:01	VVVGAGVGK	KRAS G12A



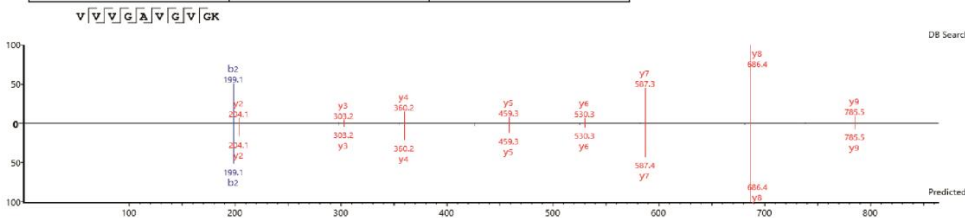
HLA Allele	Mutated Peptide	Mutated Gene
HLA-A*11:01	VVVGASGVGK	KRAS G12S



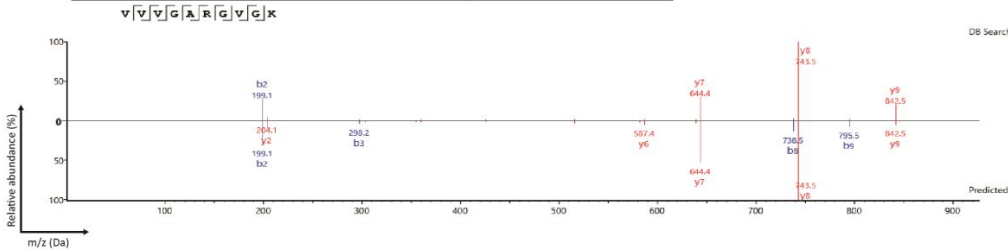
HLA Allele	Mutated Peptide	Mutated Gene
HLA-A*11:01	VVGVGVGVGK	KRAS G12V

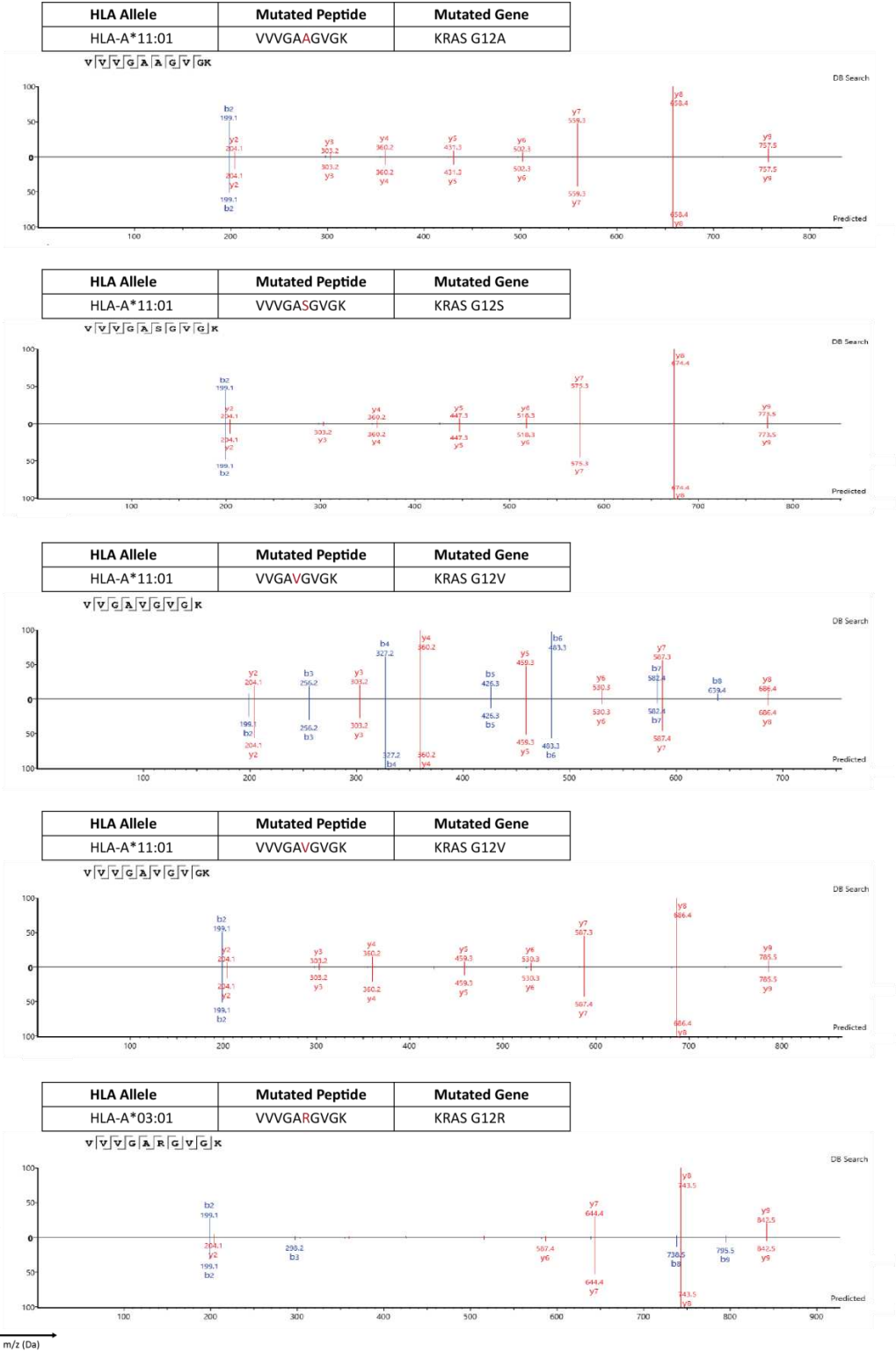


HLA Allele	Mutated Peptide	Mutated Gene
HLA-A*11:01	VVGVGVGVGK	KRAS G12V

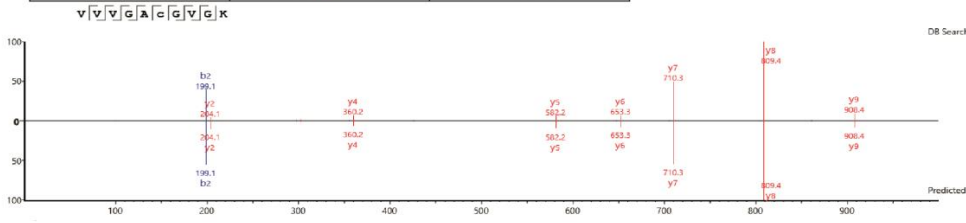


HLA Allele	Mutated Peptide	Mutated Gene
HLA-A*03:01	VVVGARGVGK	KRAS G12R

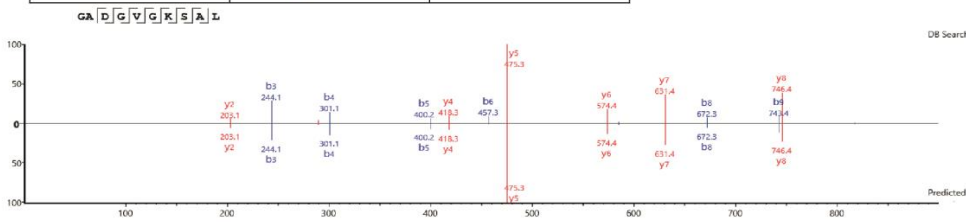




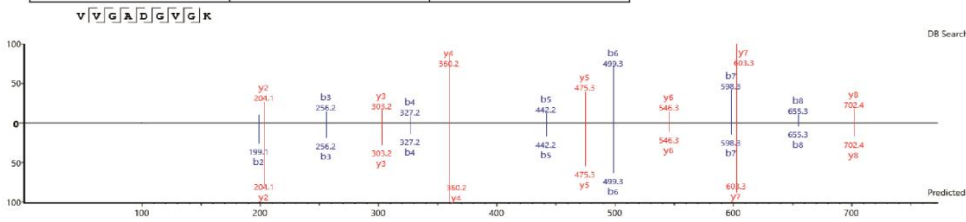
HLA Allele	Mutated Peptide	Mutated Gene
HLA-A*11:01	VVGACGVGK	KRAS G12C



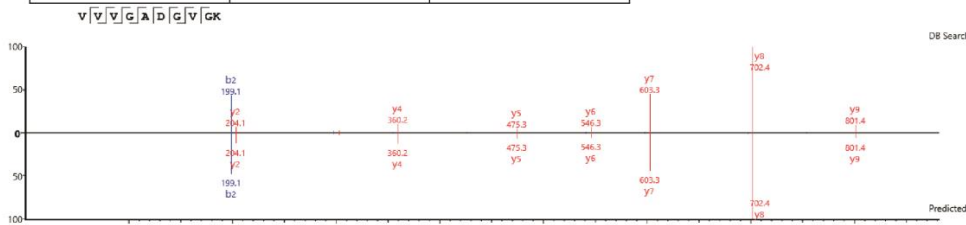
HLA Allele	Mutated Peptide	Mutated Gene
HLA-C*08:02	GADGVGKSAL	KRAS G12D



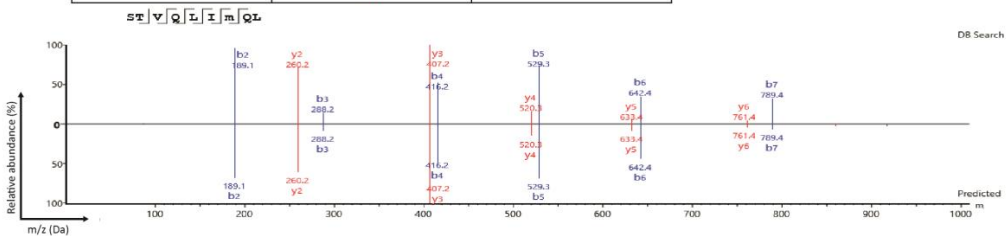
HLA Allele	Mutated Peptide	Mutated Gene
HLA-A*11:01	VVGADGVGK	KRAS G12D



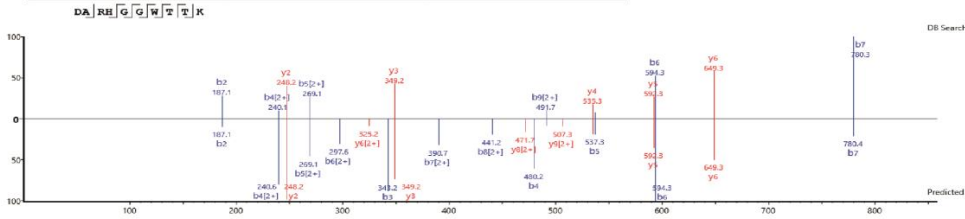
HLA Allele	Mutated Peptide	Mutated Gene
HLA-A*11:01	VVGADGVGK	KRAS G12D



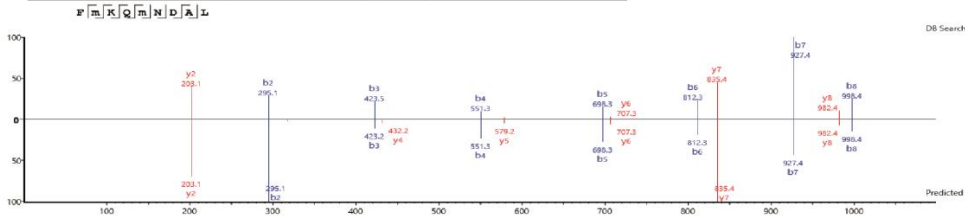
HLA Allele	Mutated Peptide	Mutated Gene
HLA-C*03:04	STVQLIMQL	EGFR T790M



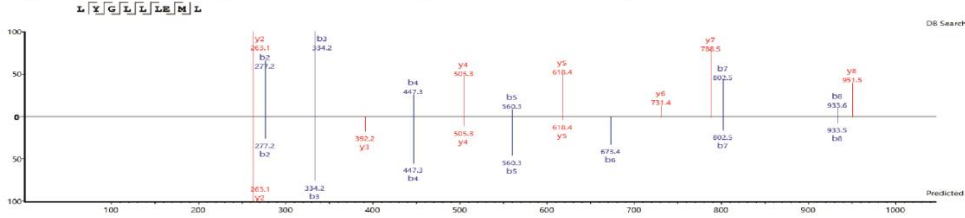
HLA Allele	Mutated Peptide	Mutated Gene
HLA-A*33:01	DARHGGWTTK	PIK3CA H1047R



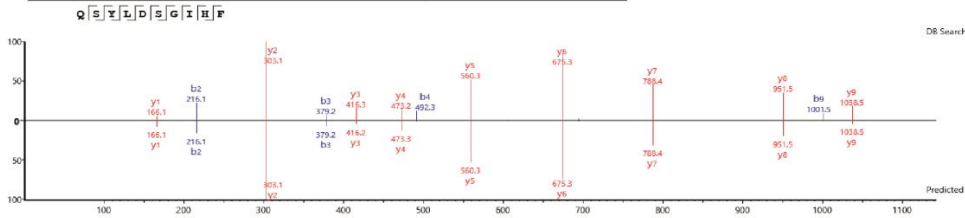
HLA Allele	Mutated Peptide	Mutated Gene
HLA-B*08:01	FMKQMNDAL	PIK3CA H1047L



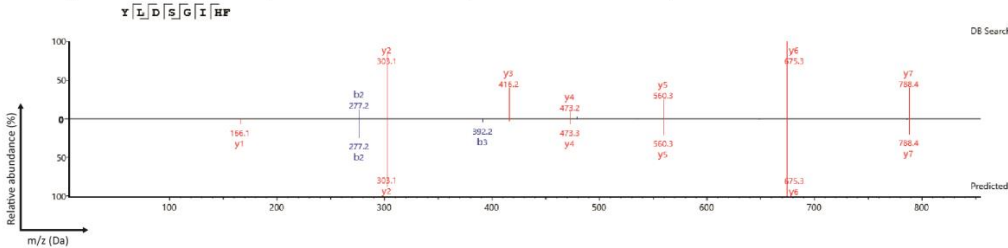
HLA Allele	Mutated Peptide	Mutated Gene
HLA-A*24:02	LYGLLLEML	ESR1 D538G

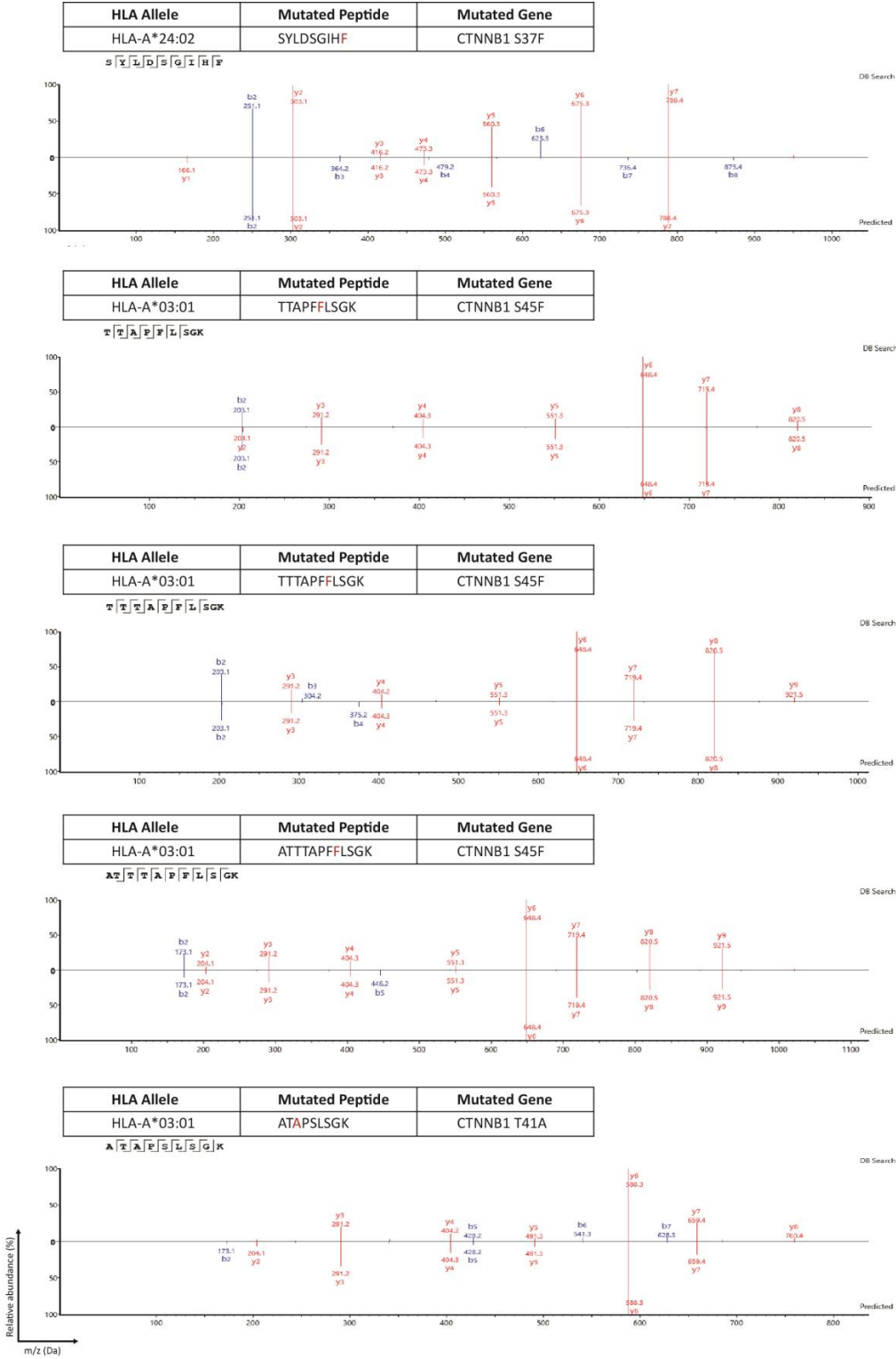


HLA Allele	Mutated Peptide	Mutated Gene
HLA-C*07:02	QSYLDSGIH F	CTNNB1 S37F

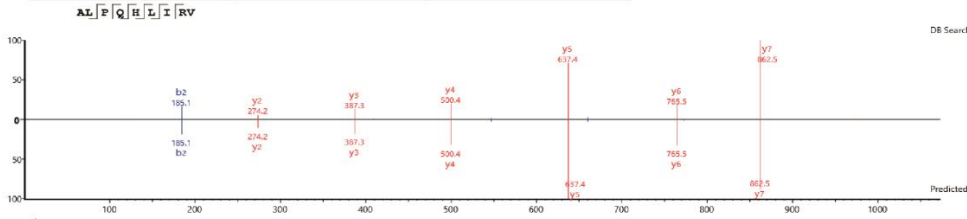


HLA Allele	Mutated Peptide	Mutated Gene
HLA-A*24:02	YLDSGIH F	CTNNB1 S37F

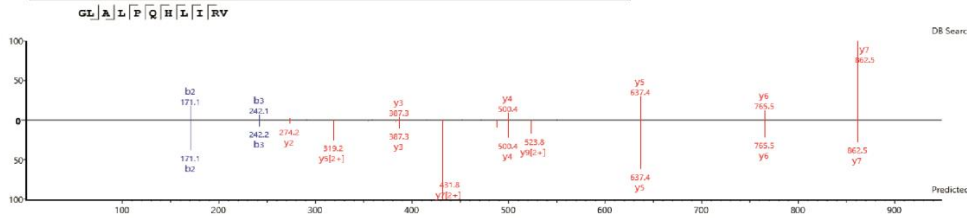




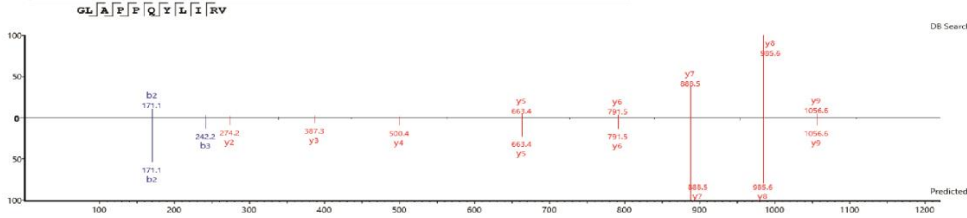
HLA Allele	Mutated Peptide	Mutated Gene
HLA-A*02:01	ALPQHILRV	TP53 P190L



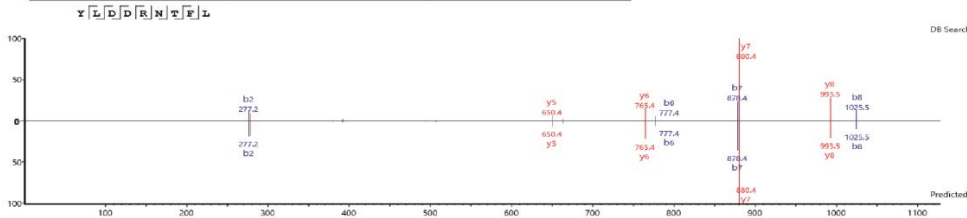
HLA Allele	Mutated Peptide	Mutated Gene
HLA-A*02:01	GLALPQHILRV	TP53 P190L



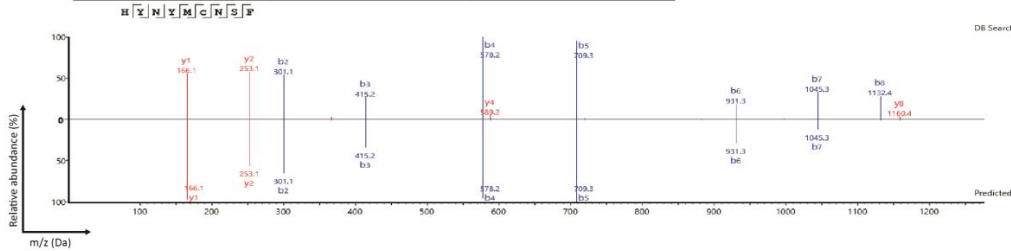
HLA Allele	Mutated Peptide	Mutated Gene
HLA-A*02:01	GLAPPQYLIRV	TP53 H193Y

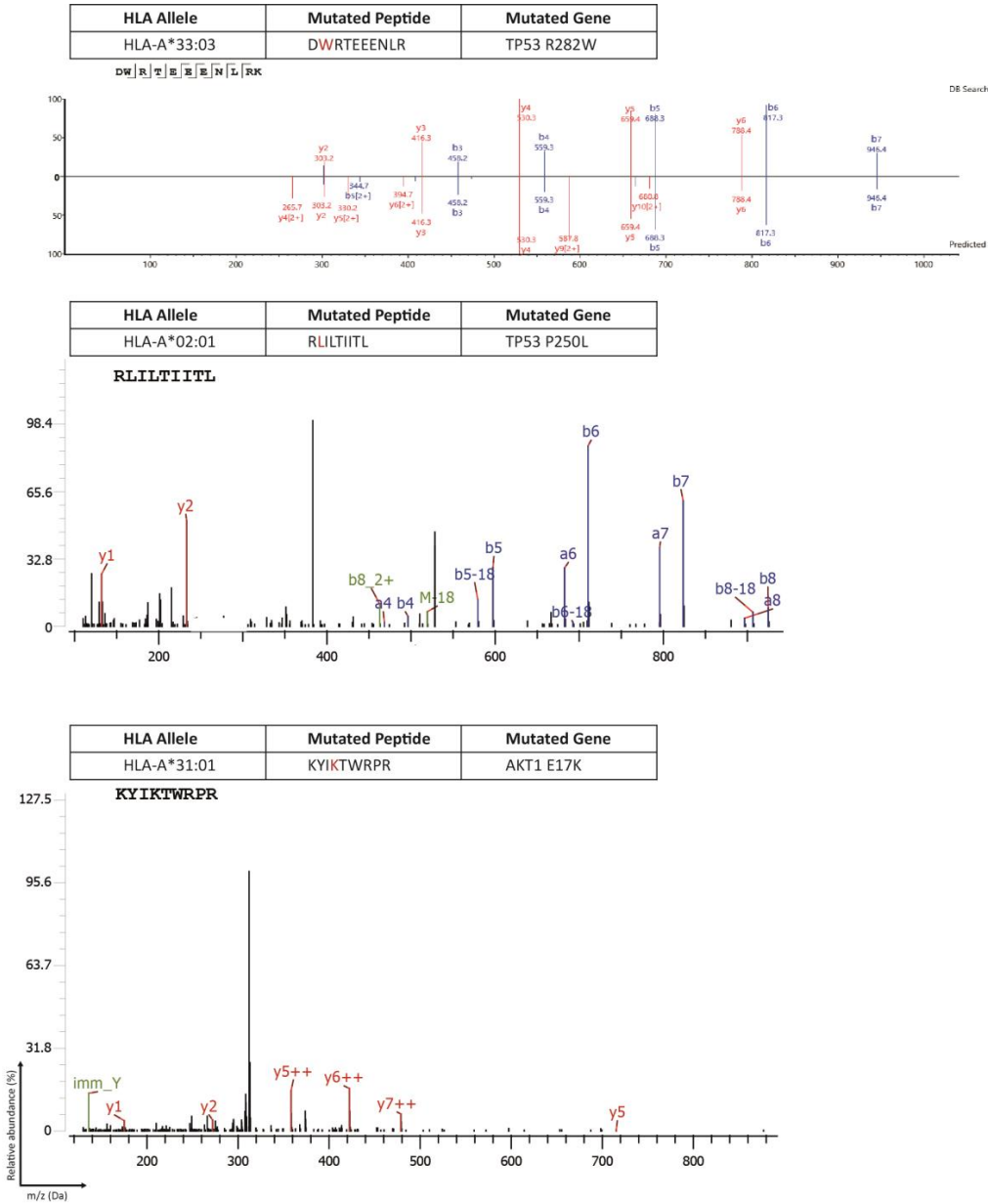


HLA Allele	Mutated Peptide	Mutated Gene
HLA-A*02:01	YLDDRNTFL	TP53 R213L

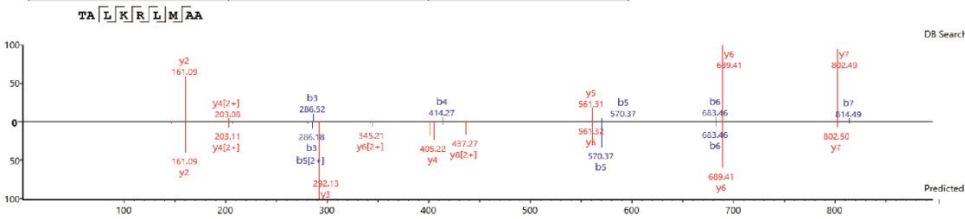


HLA Allele	Mutated Peptide	Mutated Gene
HLA-A*24:02	HYNVMCNSF	TP53 S241F

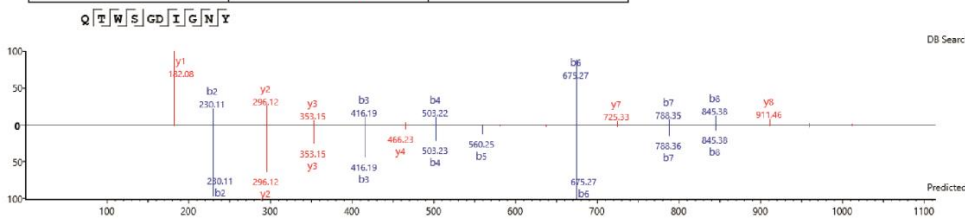




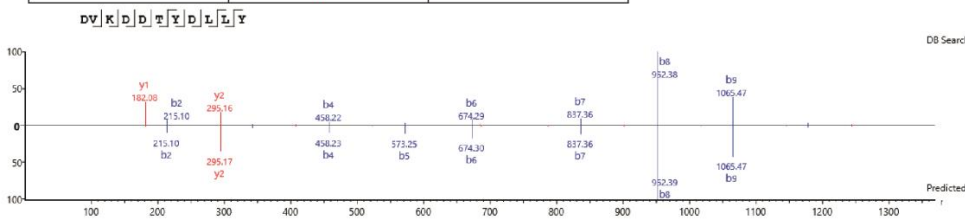
HLA Allele	Mutated Peptide	Mutated Gene
HLA-B*08:01	TALKRLMAA	UBE2G2 E12A



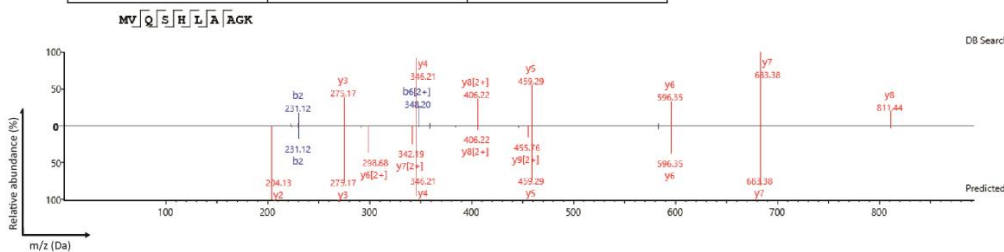
HLA Allele	Mutated Peptide	Mutated Gene
HLA-A*01:01	QTWSGDIGNY	SDK1 D644N



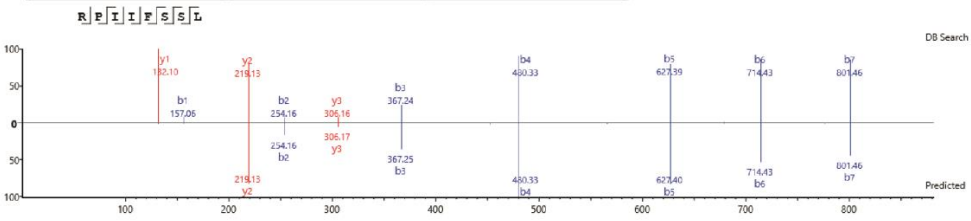
HLA Allele	Mutated Peptide	Mutated Gene
HLA-A*01:01	DVKDDTYDLLY	PRSS23 E300D



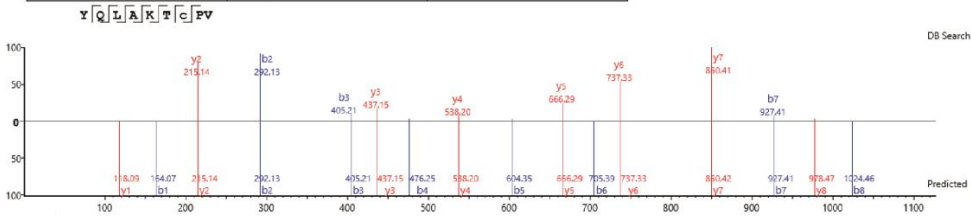
HLA Allele	Mutated Peptide	Mutated Gene
HLA-A*03:01	MVQSHLAAGK	SYT7 T133M



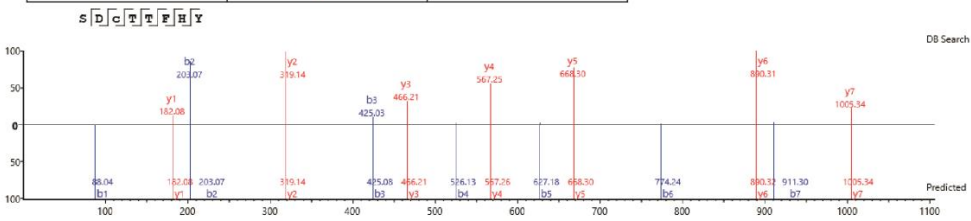
HLA Allele	Mutated Peptide	Mutated Gene
HLA-B*07:02	RPIIFSSL	TAS2R43 L5R



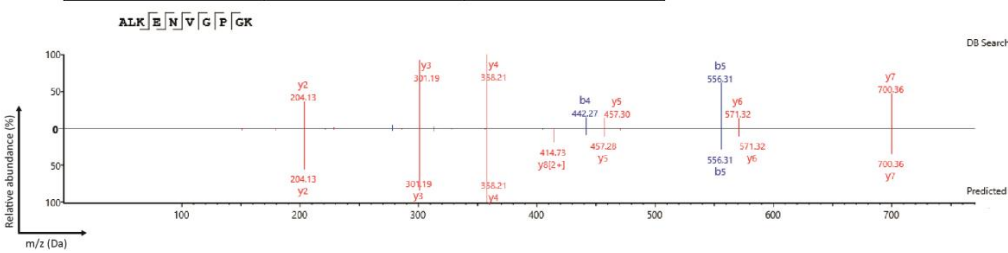
HLA Allele	Mutated Peptide	Mutated Gene
HLA-A*02:01	YQLAKTCPV	TP53 C135Y



HLA Allele	Mutated Peptide	Mutated Gene
HLA-A*01:01	SDCTTFHY	TP53 I232F



HLA Allele	Mutated Peptide	Mutated Gene
HLA-A*01:01	KSDPTEWAMY	CDO1 E41K



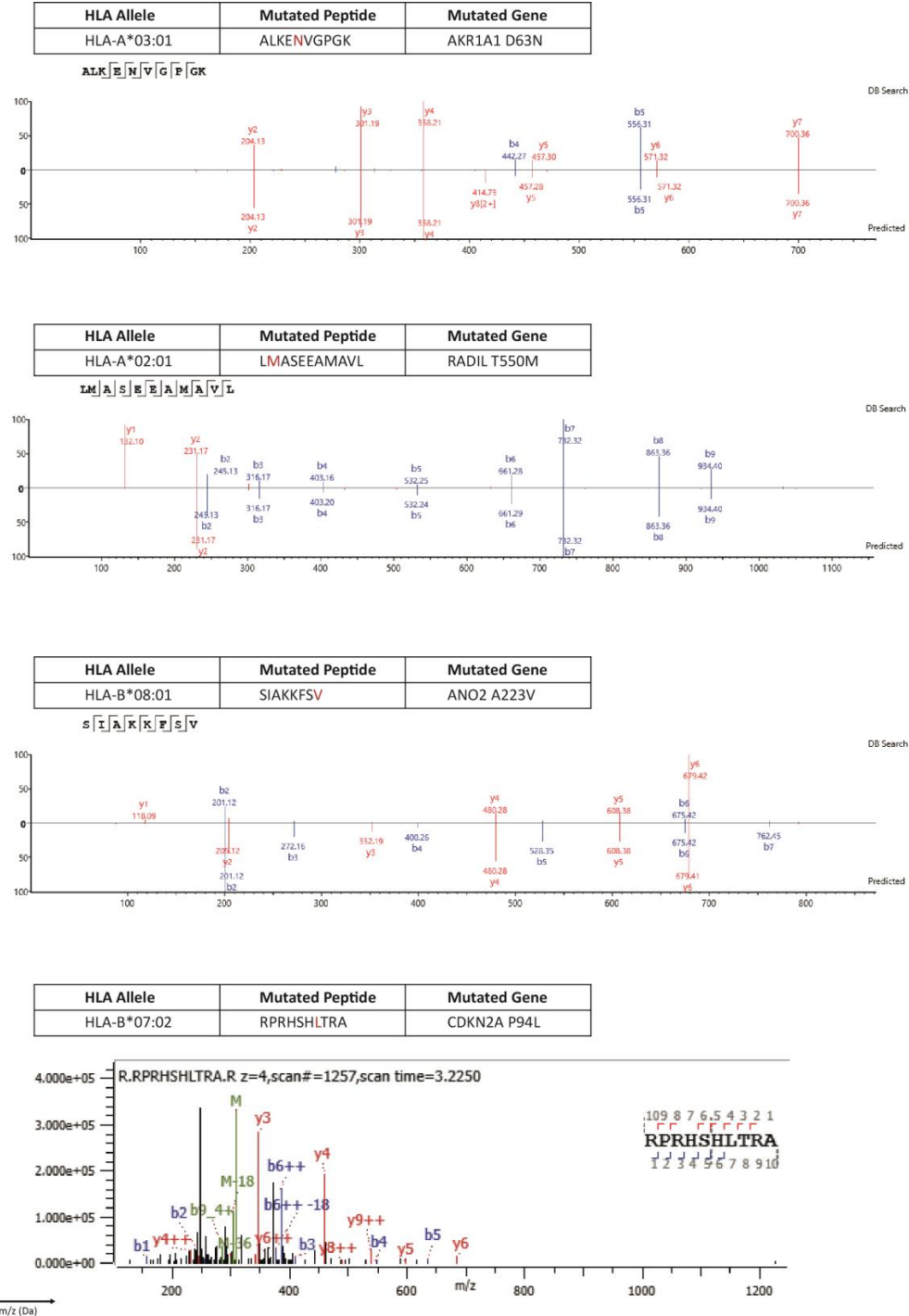
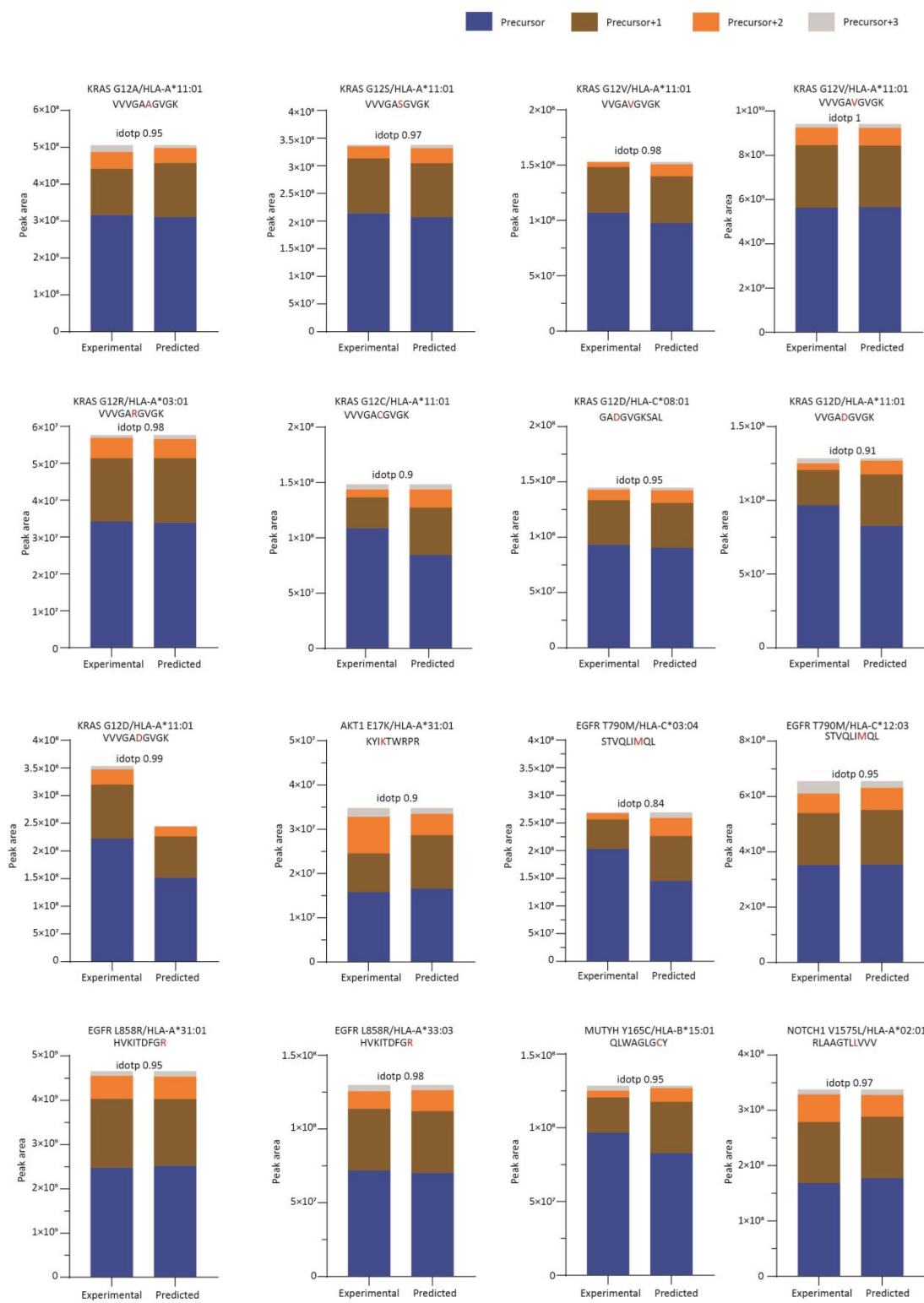
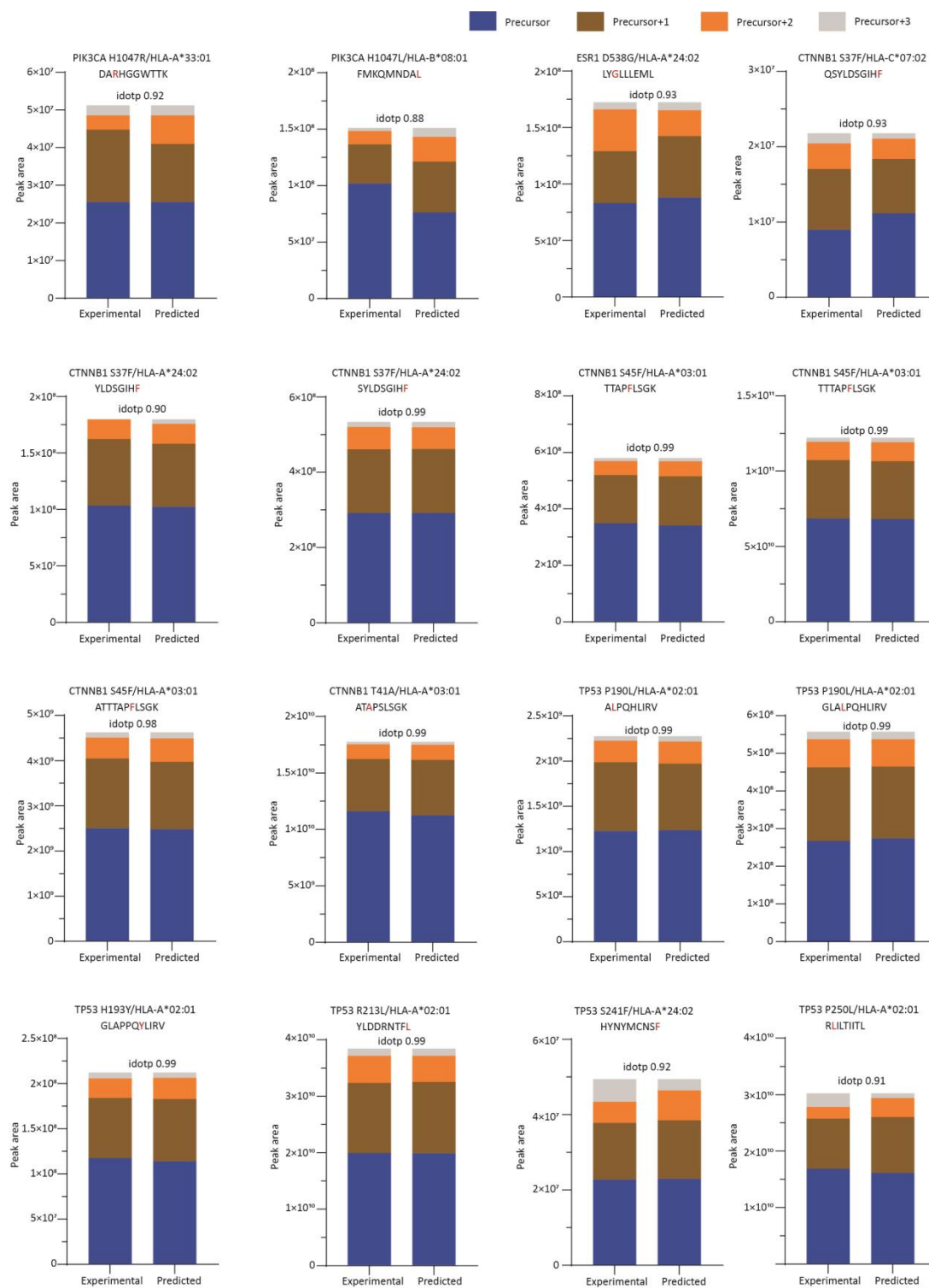


Figure S4: Mirror plots of MS2 spectra for detected neoantigens. Mirror plots showing MS2 spectra of the detected neoantigens eluted from different mutated protein/HLA combination cells (Experimental) and a predicted mirror plot (Predicted). Peaks represent b ions in blue and y ions in orange.





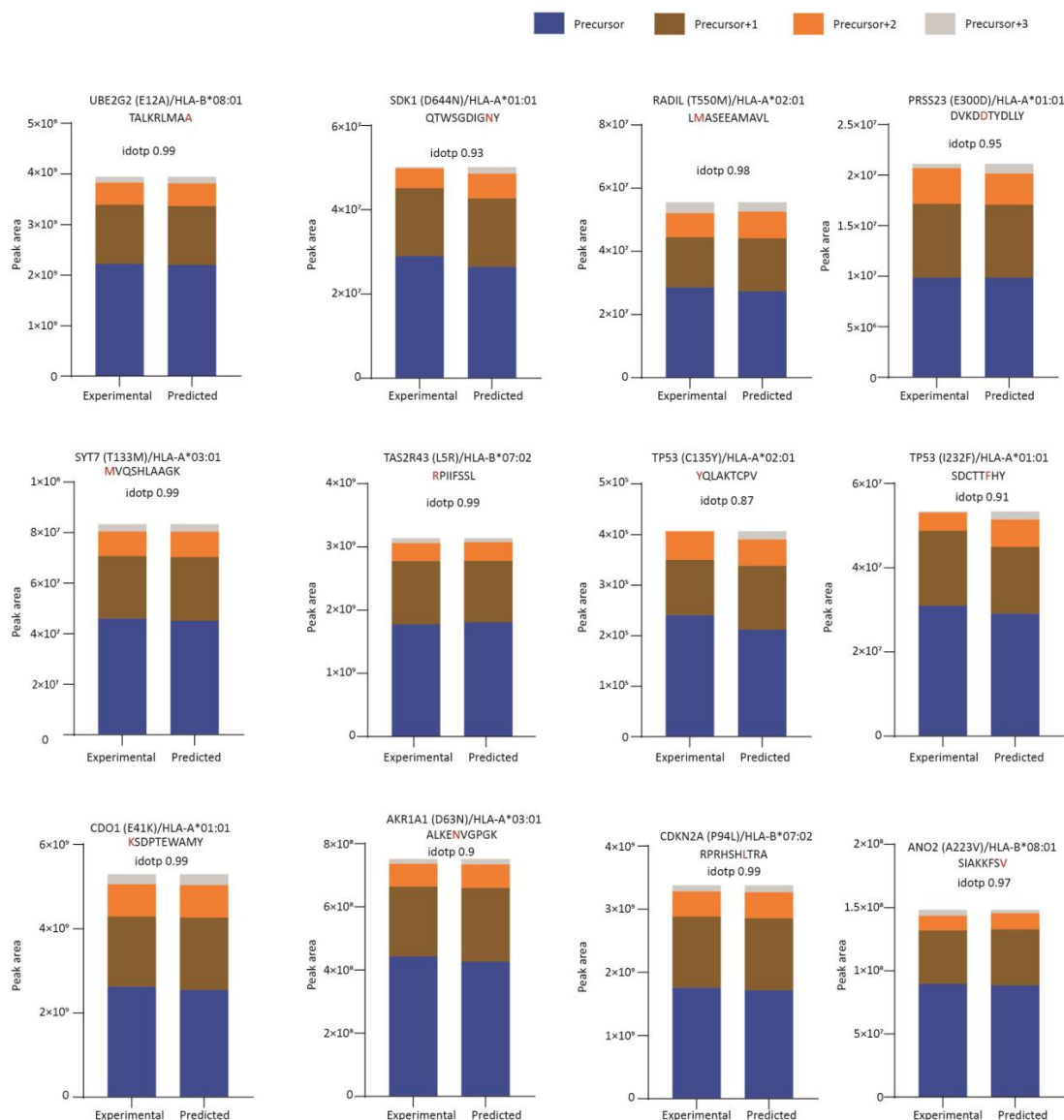


Figure S5: Skyline analysis of HLA-bound neoantigens. Relative abundance of precursor ions derived from peptides associated with the specified proteins, which were eluted from HLA mono-allelic COS-7 cell lines (Experimental). Additionally, it presents the Skyline-predicted relative distribution of isotopes of precursor ions (Predicted). “Precursor” denotes the intact peptide ion, while “+1,” “+2,” and “+3” indicate the same peptide detected in different isotopic variants. The figure also includes Idotp values, which represent the alignment of the predicted isotope pattern with the experimental observation. Values of greater than 0.9 are considered positive identifications but since these peptides were also detected with their fragmented spectra slightly smaller values are also acceptable.

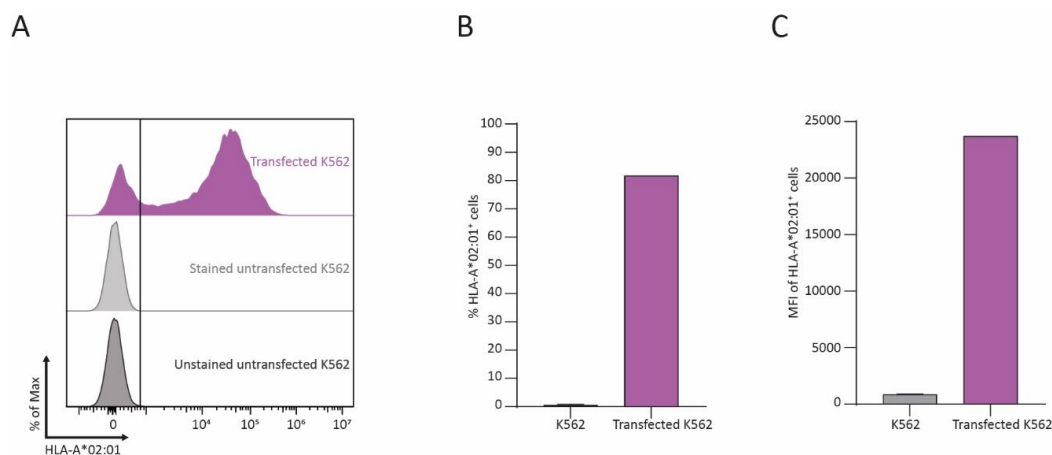


Figure S6: Transfection efficiency for a representative HLA allele (HLA-A*02:01) in K562 cells. (A) Histogram showing surface HLA-A*02:01 expression in transfected and untransfected cells. Unstained and stained untransfected K562 cells were used as negative controls. **(B)** Bar graph showing the percentage of HLA-A*02:01 in transfected and untransfected K562 cells. **(C)** Bar graph showing the MFI of HLA-A*02:01 in transfected and untransfected K562 cells.